ASME Open Journal of Engineering
Online journal at:
https://asmedigitalcollection.asme.org/openengineering

Frederick Sebastian
Department of Bioengineering,
Northeastern University,
Boston, MA 02115
e-mail: sebastian.f@northeastern.edu

Hayden DelCiello
Khoury College of Computer Sciences,
Northeastern University,
Boston, MA 02115
e-mail: delciello.h@northeastern.edu

Anup D. Pant
Department of Biomedical Engineering,
The University of Akron,
Akron, OH 44325
e-mail: pantanup@gmail.com

Michaël J. A. Girard
Mem. ASME
Department of Ophthalmology,
Emory University School of Medicine,
Atlanta, GA 30322;
Department of Biomedical Engineering,
Georgia Institute of Technology/Emory University,
Emory Empathetic AI for Health Institute,
Atlanta, GA 30322
e-mail: mgirard@ophthalmic.engineering

Vanita Pathak-Ray
Center for Sight Super Speciality Eye Hospital,
Hyderabad 500034, Telangana, India
e-mail: vpathakray@gmail.com

Syril K. Dorairaj
Department of Ophthalmology,
Mayo Clinic,
Jacksonville, FL 32224
e-mail: Dorairaj.Syril@mayo.edu

Rouzbeh Amini[1]
Mem. ASME
Department of Bioengineering,
Department of Mechanical and Industrial Engineering,
Northeastern University,
Boston, MA 02115
e-mail: r.amini@northeastern.edu

Image-Based Inverse Modeling Analysis of Iris Stiffness Across Sex in Patients With a History of Primary Angle-Closure Disease

In this study, we quantified differences in iris stiffness between female and male subjects in healthy and postlaser peripheral iridotomy (post-LPI) groups using an image-based inverse modeling approach. We analyzed anterior segment optical coherence tomography (AS-OCT) images from 25 participants across four groups. Finite element models were created using **SOLIDWORKS, **ABAQUS, *and a custom C program, modeling the iris as a neo-Hookean material. We found that post-LPI females had significantly higher normalized elastic modulus ($E' = 3.81 \pm 1.74$) than healthy females ($E' = 0.92 \pm 0.31$, $p = 0.004$), while no significant difference was observed in males. Post-LPI females also showed significantly higher stiffness than post-LPI males ($p = 0.003$). Here, p denotes the probability value, with $p < 0.05$ considered statistically significant. Our findings suggest that sex-based differences in iris biomechanics may contribute to the higher susceptibility of females to primary angle-closure disease. Despite the small sample size, this preliminary study highlights the need for larger, sex-stratified investigations into glaucoma pathophysiology.* [DOI: 10.1115/1.4068677]

Keywords: bioengineering, biomechanics, glaucoma, engineering education, eye

1 Introduction

In this study, we aimed to identify potential sex-based differences in iris stiffness through a biomechanical analysis conducted on a limited cohort of patients and healthy volunteers. Our study was driven by the significant global health and economic burden of glaucoma, a leading cause of irreversible blindness and vision impairment, which is expected to affect 112 million people by 2040 [1,2]. In 2018, the global loss in gross domestic product due to vision impairment and blindness was estimated at $411 billion [3]. Glaucoma refers to a group of diseases where increased intraocular pressure (IOP) can lead to optic nerve damage, though

[1]Corresponding author.

Manuscript received April 4, 2025; final manuscript received May 10, 2025; published online June 2, 2025. Assoc. Editor: Hameed Metghalchi.

damage may also occur without elevated IOP (normal tension glaucoma), and elevated IOP does not always cause glaucomatous damage (ocular hypertension) [4,5]. Structural damage to the optic nerve results in the irreversible loss of retinal ganglion cells, causing vision impairment [6]. The two major types of glaucoma are primary open-angle glaucoma (POAG) and primary angle-closure glaucoma (PACG). In PACG, the iris bows forward, blocking the drainage of aqueous humor through the trabecular meshwork and narrowing the anterior chamber angle (ACA), thus impeding outflow and increasing IOP (Fig. 1) [7,8].

The risk factors for glaucoma include age, ethnicity, family history, anatomy, and sex [9]. While POAG is more prevalent in regions like North America, the higher prevalence of PACG in Asian and female populations highlights its global significance [8]. Women account for 60% of all glaucoma cases worldwide [10], with factors such as longevity, hormonal changes, and anatomical predisposition contributing to this gender disparity. PACG also presents a greater burden of visual morbidity compared to POAG, with women facing a threefold higher risk than men [11].

Early diagnosis is crucial in reducing the societal and individual impact of glaucoma, as many patients are asymptomatic in the early stages [12,13]. Gonioscopy, though commonly used to assess angle closure, can be subjective and prone to misdiagnosis [14]. To improve diagnostic accuracy, techniques like ultrasound biomicroscopy (UBM) and anterior segment optical coherence tomography (AS-OCT) are employed, offering enhanced evaluation of ocular morphology, particularly in PACG cases.

Laser peripheral iridotomy (LPI) is a procedure where a laser creates small perforations in the iris to alleviate pupillary block, providing an alternate route for the aqueous humor and reducing the pressure differential between the anterior and posterior chambers [15]. Although LPI is the most common treatment for pupillary block [16], previous findings suggest that its effects may diminish over time, indicating it may not be a permanent solution [17]. Furthermore, only a fraction of individuals with narrow angles develop PACG, suggesting additional mechanisms are involved [18,19].

While UBM and AS-OCT provide detailed evaluations of the iris and anterior chamber angle, they do not directly assess iris stiffness [20]. Recent researchers have explored the biomechanical properties of the iris in relation to PACG pathophysiology [8,21,22]. For instance, Pant et al. [8] used clinical images to model how stiffer irides in PACG patients may contribute to narrowing of the anterior chamber angle in vivo, while Narayanaswamy et al. [22] demonstrated that ex vivo PACG irides exhibit significantly higher stiffness compared to healthy or POAG irides. Given the higher risk of PACG in women and the evidence linking iris stiffness to PACG, we hypothesize in this preliminary study that iris stiffness may differ between male and female eyes. Although a recent study reported sex-dependency in murine iris stiffness [23], differences between human male and female irides have yet to be identified. We aim to explore this hypothesis using an AS-OCT image-based inverse modeling approach [8].

2 Methods

2.1 Imaging and Meshing. Visante AS-OCT (Carl Zeiss Meditec, Inc., Dublin, CA) images were acquired from two groups of an Indian population at the LV Prasad Eye Institute in Hyderabad, India. The first group consisted of healthy subjects, while the second group consisted of patients who had undergone LPI for occludable ACA but continued to suffer from occludable ACA following the LPI procedure. The latter group will be referred to as the post-LPI group from this point forward. While there were at least some pathological features on gonioscopy or elevated IOP (or both) in the latter group, these individuals did not exhibit disc changes, which are criteria for PACG. As outlined by Foster et al. [24], we referred to the pathophysiology of this group as primary angle-closure (PAC) disease. This study had a total of 25 subjects: 13 female (seven healthy; six post-LPI) and 12 male (six healthy; six post-LPI). Subjects were included if they were above 18 years of age, had normal corneas, and were treatment-naïve, meaning they had no history of prior ocular hypotensive medication or surgery. For the post-LPI group, angle occludability post-LPI was established through darkroom gonioscopy with a four-mirror indentation-type gonioscope. Occludable angles were defined as iridotrabecular touch in at least 180 deg of the angle, i.e., posterior trabecular meshwork not visible for at least 180 deg of the angle. This was associated with one or more of the following features: raised IOP, peripheral anterior synechiae, or blotchy pigments. Patients with occludable angles post-LPI were included to capture a cohort where mechanisms beyond relative pupillary block may contribute to PAC. The exclusion criteria were a history of ocular surgery, trauma, uveitis, phacomorphic glaucoma, nanophthalmos, or any secondary angle closure. Cataracts were the only co-existing

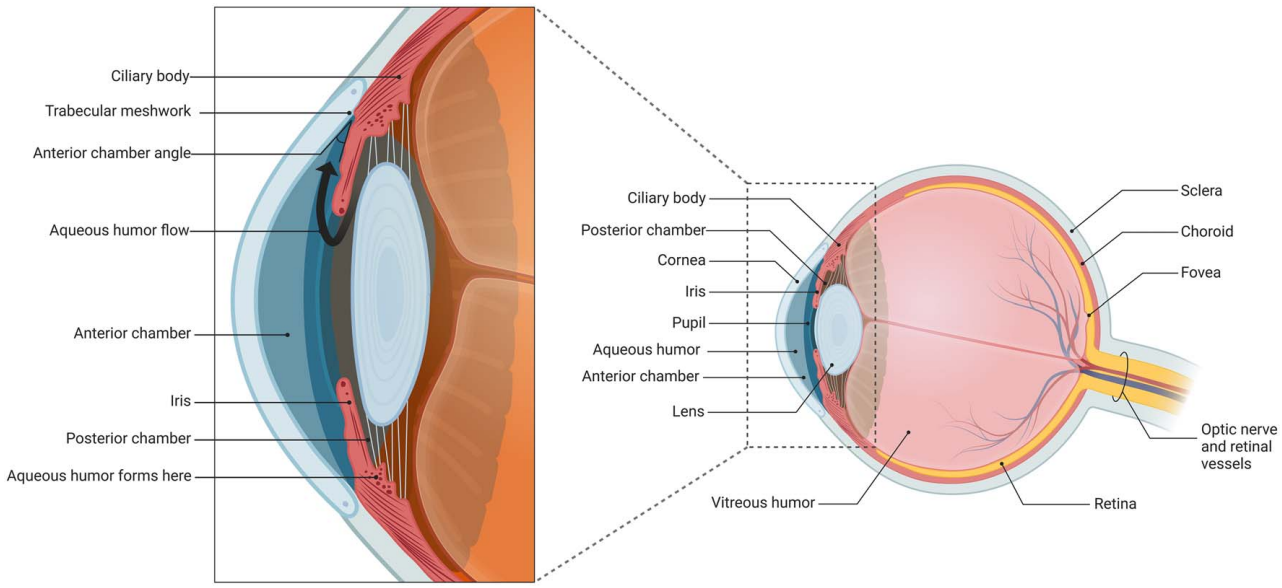

Fig. 1 Illustration highlighting the anatomical structures of the anterior eye, with a focus on the pathway of aqueous humor flow. Blockage in the aqueous humor outflow pathway, caused by obstruction at the anterior chamber angle, is commonly identified as the primary mechanism behind angle-closure glaucoma. Schematic created with Biorender.com.

Table 1 Demographic and measured parameters of the enrolled population reported as mean ± standard error where applicable

Variable	Healthy females	Post-LPI females	Healthy males	Post-LPI males
Sample size	7	6	6	6
Age (years)	53.29 ± 2.49	58.33 ± 3.95	57.00 ± 4.00	54.50 ± 4.96
Iris length in std light (mm)	4.49 ± 0.17	4.24 ± 0.14	4.44 ± 0.10	4.47 ± 0.08
Iris length in dim light (mm)	3.96 ± 0.17	4.11 ± 0.15	4.01 ± 0.07	3.94 ± 0.09
Iris thickness in std light (mm)	0.69 ± 0.02	0.75 ± 0.03	0.76± 0.03	0.76 ± 0.04
Iris thickness in dim light (mm)	0.74 ± 0.03	0.78 ± 0.04	0.80 ± 0.04	0.73 ± 0.04
ACA in std light (deg)	21.47 ± 2.29	17.26 ± 2.80	22.63 ± 1.36	13.21 ± 2.60
ACA in dim light (deg)	21.78 ± 2.27	19.36 ± 4.01	24.26 ± 2.37	15.20 ± 3.65

Note: "Std light" refers to standard light conditions.

ocular condition allowed. The sample size for this study was based on the available data from the LV Prasad Eye Institute in Hyderabad, India. While the collection of additional data for patients was limited by the recruitment challenges of human subjects, especially healthy participants, we acknowledge the need for larger sample sizes to improve the statistical power of future studies. Demographic of the patient population is presented in Table 1. The ethical principles of the Declaration of Helsinki were adhered to for this study.

The segmentation has been described in detail previously [8]. In summary, each subject's eye was imaged in standard light and followed by dim light-induced dilation. Under standard light conditions, an ambient light intensity of 350 lux was maintained without directing any light specifically toward the eye, using standard room illumination to stimulate the eye. For the dim light conditions, the 350-lux light source was switched off. Patients with an abnormal pupillary light reflex response (i.e., lack of pupil dilation) were excluded from the study. In all scans, the images were aligned and rotated to ensure the corneal axis was positioned at the center. Parameters such as ACA, iris thickness, and iris length were measured using internally developed image analysis software [25]. The image from the light conditions was measured between the iris root and tip to obtain a target distance to be used for the inverse modeling. The right side of the dilated iris was traced and meshed, using **SOLIDWORKS (Dassault Systèmes, Vélizy-Villacoublay, France) and **ABAQUS (Dassault Systèmes, Vélizy-Villacoublay, France). Within the pupillary portion of the iris, a region on the mesh of an estimated 7% volume was chosen as the sphincter region. The summarized process is presented in Fig. 2. All S8R elements from **ABAQUS were then converted to 9-node biquadratic quadrilateral elements, using **PYTHON (Python Software Foundation, Wilmington, DE).

2.2 Numerical Solution. The mathematical governing equation for light-induced iris deformation has been described in detail in our previous publications [8,26]. Briefly, the iris was modeled as a two-dimensional (axisymmetric), isotropic, neo-Hookean solid with a constant active stress applied in a single sphincter muscle region and was governed by the following stress balance equation:

$$\nabla \cdot \boldsymbol{\sigma} = 0 \tag{1}$$

with $\boldsymbol{\sigma}$ being the Cauchy stress tensor defined as the sum of the neo-Hookean stress tensor ($\boldsymbol{\sigma}_{NH}$) and the active sphincter stress tensor ($\boldsymbol{\sigma}_{Sph}$):

$$\boldsymbol{\sigma} = \boldsymbol{\sigma}_{NH} + \boldsymbol{\sigma}_{Sph} \tag{2}$$

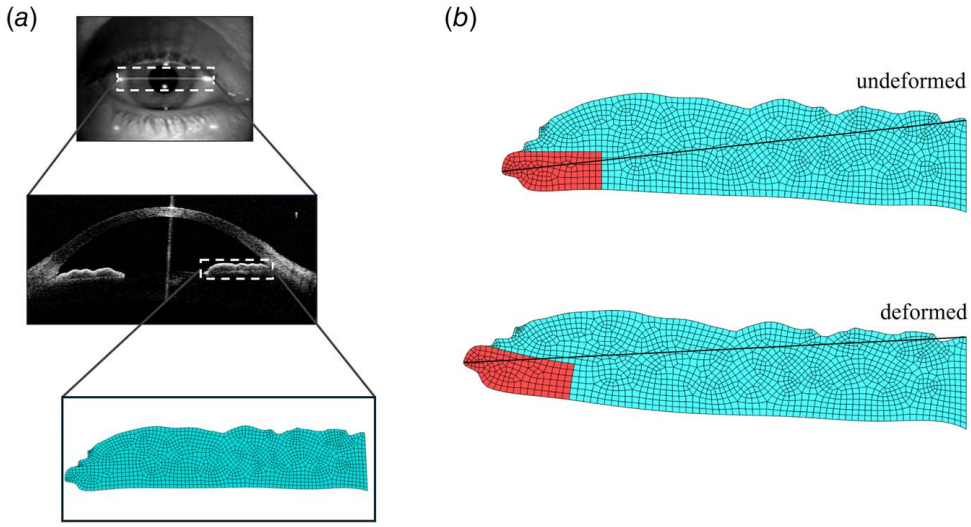

Fig. 2 (*a*) Illustration depicting the meshing process applied to a 51-year-old healthy female subject. From top to bottom: an image of the subject's eye in front of the AS-OCT device, with a highlighted region of interest delineated by a white box; AS-OCT image featuring the right portion of the iris outlined for further development in **SOLIDWORKS; and the resultant mesh representation of the iris, generated using **ABAQUS. (*B*) Simulation of iris deformation with a darker region indicating the sphincter and a line from the node to the root representing the measured iris length, *d*.

The neo-Hookean stress tensor was defined as

$$\boldsymbol{\sigma}_{\mathrm{NH}} = \frac{G}{J}(\mathbf{B} - \mathbf{I}) + \frac{2G\nu}{(1-2\nu)J}\ln(J)\mathbf{I} \tag{3}$$

$$\mathbf{B} = \mathbf{F}\mathbf{F}^{T} \tag{4}$$

$$J = \det(\mathbf{F}) \tag{5}$$

with $\mathbf{I}$ being the identity tensor, G being the shear modulus, ν being Poisson's ratio, $\mathbf{B}$ being the left Cauchy-Green deformation tensor, and J being the determinant of the deformation gradient, $\mathbf{F}$. The deformation gradient tensor was defined using $\mathbf{x}$, the position of a point on the deformed iris configuration, and $\mathbf{X}$ the position of the same point in the referential configuration:

$$\mathbf{F} = \frac{d\mathbf{x}}{d\mathbf{X}} \tag{6}$$

The active sphincter stress tensor was defined as

$$\boldsymbol{\sigma}_{\mathrm{Sph}} = \sigma_{\mathrm{Act}}\boldsymbol{e}_{\theta} \otimes \boldsymbol{e}_{\theta} \tag{7}$$

with σ_{Act} being a scalar representing the sphincter stress magnitude, and $\boldsymbol{e}_{\theta}$ the unit vector for the direction of the sphincter muscle.

To compute $\boldsymbol{\sigma}_{\mathrm{NH}}$ and $\boldsymbol{\sigma}_{\mathrm{Sph}}$ from Eqs. (3) and (7), all the variables were geometry-defined, except for the shear modulus G, Poisson's ratio ν, and the sphincter stress magnitude σ_{Act}. Based on our previous experience with a similar modeling approach [8], in all simulations we used a nearly incompressible model ($\nu = 0.49$). Additionally, we did not obtain the subjects' magnitude of sphincter stress during iris contraction, so we used a σ_{Act} of 40 kPa for all models as a physiologically reasonable estimate [8]. Varying σ_{Act} was also expected to change the calculated elastic modulus E, so simulation results were expressed as a normalized elastic modulus E', which did not significantly change with perturbations to σ_{Act} [8]:

$$E = 2G(1+\nu) \tag{8}$$

$$E' = \frac{E}{\sigma_{\mathrm{Act}}} \tag{9}$$

With ν and σ_{Act} fixed as constants, the shear modulus G was the only remaining free variable and the target of the study. The shear modulus was computed using a combination of the Galerkin finite element method and differential evolution [27]. An internally developed computer code written in C was utilized to implement the Galerkin finite element method for the spatial discretization of the mathematical model across the generated meshes [28–32]. For solving the nonlinear algebraic equations, we employed the Newton–Raphson iteration method and the direct linear solver, MUltifrontal Massively Parallel sparse direct Solver (MUMPS; University of Bordeaux, Bordeaux, Nouvelle-Aquitaine, France) [33]. Differential evolution is a genetic algorithm that minimizes a given cost function in a population of parameters as it advances through generations. For all our models, the initial population was 10 linearly spaced values for G between 1 kPa and 91 kPa, and the cost function was the absolute difference between the root-to-tip distances in the simulation d_{sim} and in the image of the subject's contracted iris d_{exp}:

$$\mathrm{Error} = |d_{\mathrm{sim}} - d_{\mathrm{exp}}| \tag{10}$$

We used a distribution-based stopping criterion [34], alongside a maximum of 50 generations for each simulation. The solution G value was chosen to be the G value from the final population that resulted in the lowest error. Any simulations that failed to satisfy the stopping criteria—i.e., the simulation reached 50 generations with a wide spread of potential shear moduli—were considered not to have converged to a single solution and thus were not used in our analysis. All simulations were conducted on Intel CPUs using 11 processes at the Northeastern University Discovery Cluster, located in the Massachusetts Green High Performance Computing Center.

2.3 Statistical Analysis. Statistical analyses were conducted in R (R Core Team). Prior to analysis, normality of the normalized elastic moduli was assessed using the Shapiro–Wilk test. Differences between groups were then evaluated using an unpaired one-tailed t-test, with significance set at $p < 0.05$. A post hoc power analysis was conducted to evaluate the statistical power of the study in detecting differences between the female and male groups within the healthy and post-LPI groups. This analysis was performed using a one-tailed t-test with a significance level of 0.05. Additionally, correlation analysis was performed to examine the relationship between age and normalized elastic modulus within healthy and post-LPI groups, separately for female and male participants. Pearson correlation coefficients and associated p-values were calculated to assess statistical significance, using a significance level of $\alpha = 0.05$. In addition, a linear regression model was applied to assess the influence of iris parameters—such as ACA, iris thickness, and iris length—under dim and standard light conditions on iris stiffness (E').

3 Results

Simulations for each subject typically took between 10 and 20 min. When comparing E' between the healthy and post-LPI groups separately for males and females, it was found that the female post-LPI group had a significantly higher E' of 3.81 ± 1.74 than that of the female healthy group, i.e., 0.92 ± 0.31 ($p = 0.004$). However, no significant difference in E' was observed in the comparison between healthy and post-LPI male groups.

In the subset of post-LPI subjects, females demonstrated a significantly higher normalized elastic modulus E' of 3.81 ± 1.74 compared to E' of 0.74 ± 0.36 obtained for males ($p = 0.003$; Fig. 3). Conversely, within the healthy cohorts, no significant difference was observed between female and male individuals. A concise summary of the comparisons among groups can be found in Table 2.

For the healthy group, the post hoc power analysis comparing female and male samples yielded a calculated effect size of 0.67, resulting in a post hoc power of 0.29. In contrast, the comparison of female and male samples in the post-LPI group showed a calculated effect size of 2.28, leading to a post hoc power of 0.98.

Despite post-LPI groups showing greater correlation factors (r) than healthy groups, our correlation analysis revealed nonsignificant associations between age and iris stiffness in all subgroup analyses. The nonsignificance of our correlation analyses is further emphasized by the large confidence intervals. The correlation factors and their respective p-values are summarized in Table 3 and the plots are presented in Fig. 4.

Table 4 presents the results of linear regression models assessing the relationship between ACA, iris length, iris thickness, and gender with E' values under dim and standard light conditions. The analysis revealed that iris length in dim light (estimate = 1.999, p-value = 0.049) and gender (male) in both dim light (estimate = −1.209, p-value = 0.038) and standard light (estimate = −1.357, p-value = 0.041) were significant predictors of E'. The negative estimates for gender indicate that male participants had lower E' values compared to females. Other parameters, such as ACA and iris thickness, were not found to be statistically significant.

4 Discussion

Women generally live longer than men, but paradoxically often report poorer health outcomes and higher hospitalization

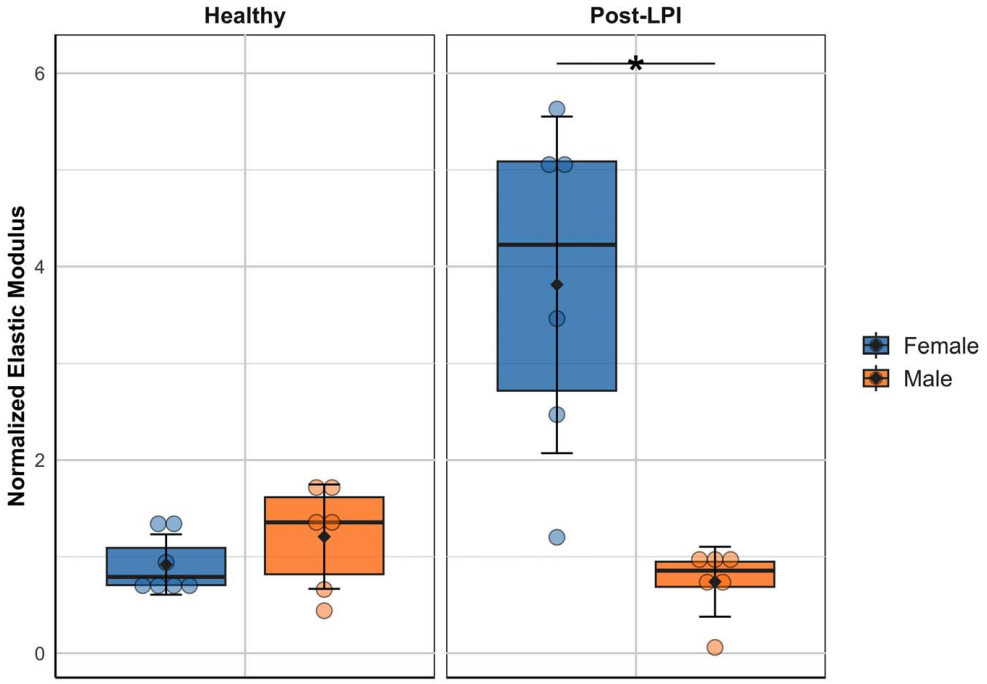

Fig. 3 Comparison of normalized elastic modulus (E') between sexes in the healthy and post-LPI groups. The diamond represents the mean value, while the asterisk and bar denote a significant difference with a *p*-value of 0.003.

Table 2 Summary of *t*-test results for the specified comparisons

Group 1	Normalized E		Group 2	Normalized E	p-Value
Healthy females	0.92 ± 0.31	vs.	Post-LPI females	3.81 ± 1.74	0.004*
Healthy males	1.21 ± 0.54	vs.	Post-LPI males	0.74 ± 0.36	0.943
Healthy females	0.92 ± 0.31	vs.	Healthy males	1.21 ± 0.54	0.858
Post-LPI females	3.81 ± 1.74	vs.	Post-LPI males	0.74 ± 0.36	0.003*

Note: Data are reported as mean ± standard error.

rates [35]. This highlights the complex interplay between sex, health, and disease, including glaucoma [36]. PACG poses a significant public health concern, with women showing a higher predisposition than men [2]. Female sex, older age, family history, and anatomical factors are major risk factors for PACG [37]. Research consistently indicates that women across all age groups have a higher risk of PACG and greater rates of vision loss compared to men [6,10]. Additionally, the burden of PACG in the aging female population may be heightened by factors such as increased collagen type 1 alpha 1 chain, the naturally shallower anterior chamber depth in females that progressively worsens with age, and menopause, which can result in an increase in IOP [38]. However, the underlying mechanisms behind the disproportionate burden of PACG on women remain unclear, underscoring the need to better understand and address sex-based disparities in the diagnosis, treatment, and management of PACG.

Table 3 Summary of correlation analysis between age and subjects for the specified groups

Group	Correlation coefficient	p-Value
Healthy females	0.09	0.86
Healthy males	0.11	0.84
Post-LPI females	0.58	0.30
Post-LPI males	0.34	0.50

Previous research using the image-based inverse modeling approach to assess iris stiffness revealed a significantly higher stiffness among irides of post-LPI subjects, compared to healthy subjects, without distinguishing between sexes [8]. Therefore, the aim of this investigation was to utilize similar methodologies to assess iris stiffness in male and female participants across both healthy and post-LPI groups. While this study is computational in nature, the estimated range of iris stiffness values is consistent with prior experimental reports, including ex vivo indentation and extension testing by Whitcomb et al. [39,40] and other experiments by Narayanaswamy et al. [22]. However, direct comparisons should be made cautiously, as experimental methods often rely on assumptions regarding boundary conditions, tissue geometry, and isotropy, which differ from the assumptions embedded within our inverse modeling framework. Despite these limitations, the alignment of computed values with experimental trends supports the plausibility of our findings.

Consistent with our proposed hypothesis, we discovered that within the post-LPI group, the iris was stiffer in female subjects compared to male subjects. However, our findings diverged from our hypothesis for the healthy group, as female iris stiffness was not significantly higher than male iris stiffness. This finding contrasts with a prior study that utilized in vivo image-based modeling with mice, which revealed a significantly higher iris stiffness in healthy female samples compared to males [23]. The discrepancy may be attributed to the small sample size in our study, with a post hoc power of 0.29 (below the standard 0.8 threshold). To

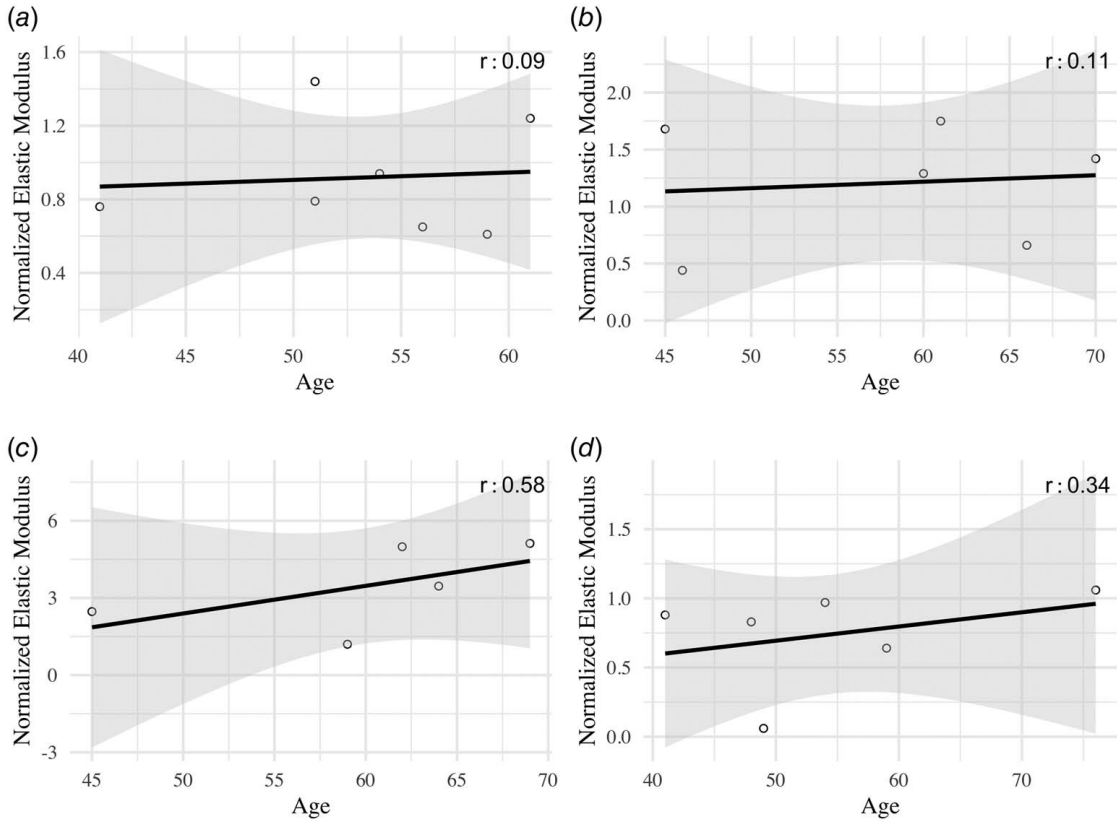

Fig. 4 Scatter plots illustrating the correlation coefficients across various tested populations

achieve 80% power, approximately 28 healthy samples per group would be required. Recruiting such a large number of healthy subjects was particularly challenging in the current human study. Therefore, future studies with larger sample sizes should be conducted to validate these findings and elucidate the underlying mechanisms driving sex-specific differences in iris stiffness.

Furthermore, our linear regression analysis suggests that sex is a more significant predictor of iris stiffness (E') than iris parameters such as ACA and thickness, particularly in the post-LPI female group. Although iris length in dim light had a modest influence, other parameters were not significant, reinforcing the idea that sex-based anatomical factors likely play a critical role in iris stiffness. These results highlight the need to consider sex-specific factors in studying primary angle-closure research. Despite these insights, the small sample size limits the generalizability of our findings. Larger cohort studies are required to fully understand the dynamics of sex differences in iris stiffness and primary angle-closure pathophysiology. Notably, post-LPI male samples did not show significantly higher E' compared to healthy males, suggesting that females may exhibit a higher prevalence of increased iris stiffness, potentially predisposing them to primary angle-closure development. Conversely, it could be argued that the biomechanical factors underlying the pathophysiology of primary angle-closure disease differ uniquely between females and males, or that females exhibit a higher prevalence of increased iris stiffness, potentially predisposing them to primary angle-closure development. This assertion is supported by our observation that post-LPI male samples did not exhibit a significantly higher E' compared to healthy male samples.

Table 4 Results of linear regression models predicting E' values based on ACA, iris length, iris thickness, and gender under dim and standard light conditions

Parameter	Estimate ± SE (dim light)	p-Value	Estimate ± SE (std light)	p-Value
Intercept	−7.509 ± 4.597	0.118	3.581 ± 5.406	0.515
ACA (deg)	−0.024 ± 0.038	0.537	−0.021 ± 0.049	0.671
Iris length (mm)	1.999 ± 0.951	0.049*	−0.546 ± 0.989	0.587
Iris thickness (mm)	2.904 ± 3.148	0.367	2.037 ± 4.129	0.627
Sex (male)	−1.209 ± 0.545	0.038*	−1.357 ± 0.623	0.041*

Note: Statistically significant parameters are marked with *. SE = standard error.

In addition to the disparities in PACG prevalence between men and women, it has been shown in a multitude of studies that PACG is an age-dependent disease [37,41–45]. Although no correlation was found between age and E' in our study, we believe that the discrepancy in relation to previous works may be attributed to the small range in age difference in our subject pool, with the average age spanning only approximately 5 years, in addition to the small sample size.

Quantifying iris stiffness in vivo comes with difficulties and limitations. The iris model used in this study was isotropic and homogeneous, significantly decreasing the actual complexity of the iris, which consists of multiple layered materials with varying mechanical properties, such as the stroma and the dilator muscle. Additionally, iris contraction was simplified from a combined contraction and relaxation of the dilator and sphincter muscles to just a contraction of the sphincter muscle, which was assumed to have a similar magnitude in all subjects. However, using the same active stress for both men and women, as well as for normal and post-LPI cases, may overlook physiological differences in muscle response and biomechanics across these groups, potentially limiting the accuracy of the model in capturing sex-specific and disease-specific variations. It is possible that LPI alone could have triggered a remodeling response in the iris tissue, and that this response may have differed between males and females. Despite the limitations of our study, we have, to our knowledge, demonstrated for the first

time that in vivo iris stiffness is significantly greater in female subjects with a history of primary angle-closure disease. Further research is warranted to explore these findings and their implications for understanding the pathophysiology of primary angle-closure disease.

5 Conclusion

In this study, we investigated sex-based differences in iris biomechanics among healthy individuals and those with a history of primary angle-closure disease treated with laser peripheral iridotomy. Using an image-based inverse modeling approach and anterior segment optical coherence tomography imaging data, we found that post-LPI females exhibited significantly greater iris stiffness than both healthy females and post-LPI males. No significant differences were observed among the healthy groups, suggesting that the remodeling response to LPI—or the underlying pathophysiology of primary angle-closure disease itself—may differ between sexes. Our regression analysis further supports the relevance of sex as an independent predictor of iris stiffness, beyond commonly measured anatomical features like iris thickness or anterior chamber angle. These findings underscore the importance of incorporating sex-specific considerations in future glaucoma research and clinical strategies. While limited by a small sample size, this work represents a critical first step in identifying biomechanical contributors to sex disparities in primary angle-closure disease and motivates larger, longitudinal studies to validate and expand upon these results.

Acknowledgment

Acknowledgment is made to the donors of the National Glaucoma Research, a program of The BrightFocus Foundation, for partial support of this research (grant number G2018177). Support for the educational component in this work was provided in part by an award from the National Science Foundation (CAREER 2049088). The schematic in Fig. 1 was generated using Biorender.com.

Conflict of Interest

All procedures performed for studies involving human participants were in accordance with the ethical standards stated in the 1964 Declaration of Helsinki and its later amendments or comparable ethical standards. Informed consent was obtained from all participants. Documentation provided upon request. This article does not include any research in which animal participants were involved.

Data Availability Statement

The datasets generated and supporting the findings of this article are obtainable from the corresponding author upon reasonable request.

Appendix

In line with our recent publications [36,46–53], we have included an educational "homework assignment" in this appendix to enhance engagement and comprehension of the methods employed in this research. This assignment is designed to be accessible to anyone with some programming experience. It centers on the concept of using "inverse modeling" to computationally determine physical parameters.

Problem—Consider a linear spring that is 10 cm long in an unloaded configuration. Under a 5 kN tensile load, it stretches to 13 cm in length. Using the programming language of your choice, implement a genetic algorithm to solve for the spring constant. You will need to:

(1) Define an initial population of trial spring constants.
(2) Decide on a cost function, a function that is minimized as the trial spring constant approaches the true spring constant. You should not just compare it to the analytical solution for the spring constant.
(3) Design a mutation strategy, a method to update trial spring constants, such that the updated trial constants favor the values that resulted in the lowest costs from the previous generation. Here are some guiding points:
    (a) The magnitude of mutation should relate to the spread of the population.
    (b) Trial spring constants that result in a low cost function value should change less between generations.
(4) Add stopping criteria, the conditions by which the algorithm stops.

For this exercise, use an initial population of 10 spring constants, between 100,000 N/m and 200,000 N/m. Compare the final population of your algorithm to the analytical solution.

References

[1] GBD 2019 Blindness and Vision Impairment Collaborators, 2021, "Causes of Blindness and Vision Impairment in 2020 and Trends Over 30 Years, and Prevalence of Avoidable Blindness in Relation to Vision 2020: The Right to Sight: An Analysis for the Global Burden of Disease Study," Lancet Global Health, **9**(2), pp. e144–e160.

[2] Tham, Y.-C., Li, X., Wong, T. Y., Quigley, H. A., Aung, T., and Cheng, C.-Y., 2014, "Global Prevalence of Glaucoma and Projections of Glaucoma Burden Through 2040: A Systematic Review and Meta-analysis," Ophthalmology, **121**(11), pp. 2081–2090.

[3] Marques, A. P., Ramke, J., Cairns, J., Butt, T., Zhang, J. H., Muirhead, D., Jones, I., et al., 2021, "Global Economic Productivity Losses From Vision Impairment and Blindness," Eclinicalmedicine, **35**, p. 100852.

[4] Anderson, D. R., Drance, S. M., Schulzer, M., and Collaborative Normal-Tension Glaucoma Study Group, 2001, "Natural History of Normal-Tension Glaucoma," Ophthalmology, **108**(2), pp. 247–253.

[5] Friedman, D. S., Wilson, M. R., Liebmann, J. M., Fechtner, R. D., and Weinreb, R. N., 2004, "An Evidence-Based Assessment of Risk Factors for the Progression of Ocular Hypertension and Glaucoma," Am. J. Ophthalmol., **138**(3), pp. 19–31.

[6] Zhang, N., Wang, J., Chen, B., Li, Y., and Jiang, B., 2021, "Prevalence of Primary Angle Closure Glaucoma in the Last 20 Years: A Meta-analysis and Systematic Review," Front. Med., **7**, p. 624179.

[7] Roberts, C. J., Downs, J. C., and Dupps, W. J., Jr., 2018, *Biomechanics of the Eye*, 1st ed., Kugler Publications, Amsterdam.

[8] Pant, A. D., Gogte, P., Pathak-Ray, V., Dorairaj, S. K., and Amini, R., 2018, "Increased Iris Stiffness in Patients With a History of Angle-Closure Glaucoma: An Image-Based Inverse Modeling Analysis," Invest. Ophthalmol. Visual Sci., **59**(10), pp. 4134–4142.

[9] Tehrani, S., 2015, "Gender Difference in the Pathophysiology and Treatment of Glaucoma," Curr. Eye Res., **40**(2), pp. 191–200.

[10] Vajaranant, T. S., Nayak, S., Wilensky, J. T., and Joslin, C. E., 2010, "Gender and Glaucoma: What We Know and What We Need to Know," Curr. Opin. Ophthalmol., **21**(2), pp. 91–99.

[11] Wright, C., Tawfik, M. A., Waisbourd, M., and Katz, L. J., 2016, "Primary Angle-Closure Glaucoma: An Update," Acta Ophthalmol., **94**(3), pp. 217–225.

[12] Stein, J. D., Khawaja, A. P., and Weizer, J. S., 2021, "Glaucoma in Adults—Screening, Diagnosis, and Management: A Review," J. Am. Med. Assoc., **325**(2), pp. 164–174.

[13] Prum, B. E., Rosenberg, L. F., Gedde, S. J., Mansberger, S. L., Stein, J. D., Moroi, S. E., Herndon, L. W., Lim, M. C., and Williams, R. D., 2016, "Primary Open-Angle Glaucoma Preferred Practice Pattern Guidelines," Ophthalmology, **123**(1), pp. P41–P111.

[14] Varma, D. K., Simpson, S. M., Rai, A. S., and Ahmed, I. I. K., 2017, "Undetected Angle Closure in Patients With a Diagnosis of Open-Angle Glaucoma," Can. J. Ophthalmol., **52**(4), pp. 373–378.

[15] Ritch, R., Tham, C. C., Spaeth, G. L., Danesh-Meyer, H. V., Goldberg, I., and Kampik, A., 2011, "Laser Peripheral Iridotomy and Iridoplasty," *Ophthalmic Surgery: Principles and Practice E-Book*, 4th ed., W.B. Saunders, London, p. 308.

[16] Ophthalmic Procedures Assessment, 1994, "Laser Peripheral Iridotomy for Pupillary-Block Glaucoma," Ophthalmology, **101**(10), pp. 1749–1758.

[17] Jiang, Y., Chang, D. S., Zhu, H., Khawaja, A. P., Aung, T., Huang, S., and Chen, Q., et al., 2014, "Longitudinal Changes of Angle Configuration in Primary Angle-Closure Suspects: The Zhongshan Angle-Closure Prevention Trial," Ophthalmology, **121**(9), pp. 1699–1705.

[18] Congdon, N. G., Youlin, Q., Quigley, H., Hung, P. T., Wang, T., Ho, T., and Tielsch, J. M., 1997, "Biometry and Primary Angle-Closure Glaucoma Among Chinese, White, and Black Populations," Ophthalmology, **104**(9), pp. 1489–1495.

[19] Wilensky, J. T., Kaufman, P. L., Frohlichstein, D., Gieser, D. K., Kass, M. A., Ritch, R., and Anderson, R., 1993, "Follow-Up of Angle-Closure Glaucoma Suspects," Am. J. Ophthalmol., **115**(3), pp. 338–346.
[20] See, J. L. S., 2009, "Imaging of the Anterior Segment in Glaucoma," Clin. Exp. Ophthalmol., **37**(5), pp. 506–513.
[21] Panda, S. K., Tan, R. K. Y., Tun, T. A., Buist, M. L., Nongpiur, M., Baskaran, M., Aung, T., and Girard, M. J. A., 2021, "Changes in Iris Stiffness and Permeability in Primary Angle Closure Glaucoma," Invest. Ophthalmol. Visual Sci., **62**(13), pp. 29–29.
[22] Narayanaswamy, A., Nai, M. H., Nongpiur, M. E., Htoon, H. M., Thomas, A., Sangtam, T., Lim, C. T., Wong, T. T., and Aung, T., 2019, "Young's Modulus Determination of Normal and Glaucomatous Human Iris," Invest. Ophthalmol. Visual Sci., **60**(7), pp. 2690–2695.
[23] Lee, C., Li, G., Stamer, W. D., and Ethier, C. R., 2021, "In Vivo Estimation of Murine Iris Stiffness Using Finite Element Modeling," Exp. Eye Res., **202**, p. 108374.
[24] Foster, P. J., Buhrmann, R., Quigley, H. A., and Johnson, G. J., 2002, "The Definition and Classification of Glaucoma in Prevalence Surveys," Br. J. Ophthalmol., **86**(2), pp. 238–242.
[25] Dorairaj, S., Pant, A., Calhoun, J., and Amini, R., 2015, "Quantitative Analysis of Anterior Segment Biometric Parameters in Controlled Light Conditions After Laser Peripheral Iridotomy," Invest. Ophthalmol. Visual Sci., **56**(7), pp. 4999–4999.
[26] Pant, A. D., Dorairaj, S. K., and Amini, R., 2018, "Appropriate Objective Functions for Quantifying Iris Mechanical Properties Using Inverse Finite Element Modeling," ASME J. Biomech. Eng., **140**(7), p. 074502.
[27] Storn, R., and Price, K., 1997, "Differential Evolution—A Simple and Efficient Heuristic for Global Optimization Over Continuous Spaces," J. Global Optim., **11**(4), pp. 341–359.
[28] Amini, R., Whitcomb, J. E., Al-Qaisi, M. K., Akkin, T., Jouzdani, S., Dorairaj, S., Prata, T., et al., 2012, "The Posterior Location of the Dilator Muscle Induces Anterior Iris Bowing During Dilation, Even in the Absence of Pupillary Block," Invest. Ophthalmol. Visual Sci., **53**(3), pp. 1188–1194.
[29] Jouzdani, S., Amini, R., and Barocas, V. H., 2013, "Contribution of Different Anatomical and Physiologic Factors to Iris Contour and Anterior Chamber Angle Changes During Pupil Dilation: Theoretical Analysis," Invest. Ophthalmol. Visual Sci., **54**(4), pp. 2977–2984.
[30] Pant, A. D., Kagemann, L., Schuman, J. S., Sigal, I. A., and Amini, R., 2017, "An Image-Based Inverse Finite Element Method to Determine In Vivo Mechanical Properties of the Human Trabecular Meshwork," J. Model. Ophthalmol., **1**(3), p. 100.
[31] Amini, R., and Barocas, V., 2010, "Reverse Pupillary Block Slows Iris Contour Recovery From Corneoscleral Indentation," ASME J. Biomech. Eng., **132**(7), p. 071010.
[32] Amini, R., Jouzdani, S., and Barocas, V. H., 2012, "Increased Iris–Lens Contact Following Spontaneous Blinking: Mathematical Modeling," J. Biomech., **45**(13), pp. 2293–2296.
[33] Amestoy, P., Duff, I., and L'Excellent, J.-Y., 2000, "Multifrontal Parallel Distributed Symmetric and Unsymmetric Solvers," Comput. Methods Appl. Mech. Eng., **184**(2), pp. 501–520.
[34] Zielinski, K., and Laur, R., 2008, *Stopping Criteria for Differential Evolution in Constrained Single-Objective Optimization*, Springer, Berlin, pp. 111–138.
[35] Hossin, M. Z., 2021, "The Male Disadvantage in Life Expectancy: Can We Close the Gender Gap?" Int. Health, **13**(5), pp. 482–484.
[36] Sebastian, F., Vargas, A. I., Clarin, J., Hurgoi, A., and Amini, R., 2023, "Meta Data Analysis of Sex Distribution of Study Samples Reported in Summer Biomechanics, Bioengineering, and Biotransport Annual Conference Abstracts," ASME J. Biomech. Eng., **146**(6), p. 060906.
[37] Sun, X., Dai, Y., Chen, Y., Yu, D.-Y., Cringle, S. J., Chen, J., Kong, X., Wang, X., and Jiang, C., 2017, "Primary Angle Closure Glaucoma: What We Know and What We Don't Know," Prog. Retinal Eye Res., **57**, pp. 26–45.
[38] Douglass, A., Dattilo, M., and Feola, A. J., 2023, "Evidence for Menopause as a Sex-Specific Risk Factor for Glaucoma," Cell. Mol. Neurobiol., **43**(1), pp. 79–97.
[39] Whitcomb, J. E., Barnett, V. A., Olsen, T. W., and Barocas, V. H., 2009, "Ex Vivo Porcine Iris Stiffening Due to Drug Stimulation," Exp. Eye Res., **89**(4), pp. 456–461.
[40] Whitcomb, J. E., Amini, R., Simha, N. K., and Barocas, V. H., 2011, "Anterior–Posterior Asymmetry in Iris Mechanics Measured by Indentation," Exp. Eye Res., **93**(4), pp. 475–481.
[41] He, M., Foster, P. J., Ge, J., Huang, W., Zheng, Y., Friedman, D. S., Lee, P. S., and Khaw, P. T., 2006, "Prevalence and Clinical Characteristics of Glaucoma in Adult Chinese: A Population-Based Study in Liwan District, Guangzhou," Invest. Ophthalmol. Visual Sci., **47**(7), pp. 2782–2788.
[42] He, M., Foster, P. J., Johnson, G. J., and Khaw, P. T., 2006, "Angle-Closure Glaucoma in East Asian and European People. Different Diseases?" EYE, **20**(1), pp. 3–12.
[43] Liang, Y., Friedman, D. S., Zhou, Q., Yang, X. H., Sun, L. P., Guo, L., Chang, D. S., Lian, L., Wang, N. L., and Handan Eye Study Group, 2011, "Prevalence and Characteristics of Primary Angle-Closure Diseases in a Rural Adult Chinese Population: The Handan Eye Study," Invest. Ophthalmol. Visual Sci., **52**(12), pp. 8672–8679.
[44] Yamamoto, T., Iwase, A., Araie, M., Suzuki, Y., Abe, H., Shirato, S., Kuwayama, Y., et al., 2005, "The Tajimi Study Report 2: Prevalence of Primary Angle Closure and Secondary Glaucoma in a Japanese Population," Ophthalmology, **112**(10), pp. 1661–1669.
[45] Foster, P. J., Baasanhu, J., Alsbirk, P. H., Munkhbayar, D., Uranchimeg, D., and Johnson, G. J., 1996, "Glaucoma in Mongolia: A Population-Based Survey in Hövsgöl Province, Northern Mongolia," Arch. Ophthalmol., **114**(10), pp. 1235–1241.
[46] Thomas, V. S., Lai, V., and Amini, R., 2019, "A Computational Multi-scale Approach to Investigate Mechanically-Induced Changes in Tricuspid Valve Anterior Leaflet Microstructure," Acta Biomater., **94**, pp. 524–535.
[47] Pakzadmanesh, M., Salinas, S. D., Thomas, V. S., Jennings, T., DelCiello, H., Vargas, A. I., Clarin, J., and Amini, R., 2024, "Mechanically Induced Deformation of Nuclei in the Tricuspid Valve Interstitial Cells: Experimental Measurements and Multi-scale Computational Simulation," ASME Open J. Eng., **3**, p. 031023.
[48] Vargas, A. I., Tarraf, S. A., Fitzgibbons, T. P., Bellini, C., and Amini, R., 2023, "Biomechanical Remodeling of the Murine Descending Thoracic Aorta During Late-Gestation Pregnancy," Curr. Res. Physiol., **7**, p. 100102.
[49] Clarin, J., Dang, D., Santos, L., and Amini, R., 2023, "Mechanical Characterization of Porcine Tricuspid Valve Anterior Leaflets Over Time: Applications to Ex Vivo Studies," ASME Open J. Eng., **2**, p. 021032.
[50] Nwotchouang, B. S. T., Eppelheimer, M. S., Biswas, D., Pahlavian, S. H., Zhong, X., Oshinski, J. N., Barrow, D. L., Amini, R., and Loth, F., 2021, "Accuracy of Cardiac-Induced Brain Motion Measurement Using Displacement-Encoding With Stimulated Echoes (Dense) Magnetic Resonance Imaging (MRI): A Phantom Study," Magn. Res. Med., **85**(3), pp. 1237–1247.
[51] Vargas, A. I., Tarraf, S. A., Jennings, T., Bellini, C., and Amini, R., 2024, "Vascular Remodeling During Late-Gestation Pregnancy: An In-Vitro Assessment of the Murine Ascending Thoracic Aorta," ASME J. Biomech. Eng., **146**(7), p. 071004.
[52] Jennings, T., Amini, R., and Müftü, S., 2025, "Toward a Consistent Framework for Describing the Free Vibration Modes of the Brain," ASME J. Biomech. Eng., **147**(4), p. 044501.
[53] Jennings, T., Tillman, A., Mukasa, D., Marchev, M., Müftü, S., and Amini, R., 2025, "Measurement and Assessment of Head-to-Helmet Contact Forces," Ann. Biomed. Eng., **53**(4), pp. 946–955.